HHS Public Access

Author manuscript

Oncogene. Author manuscript; available in PMC 2015 June 15.

Published in final edited form as:

Oncogene. 2014 March 13; 33(11): 1359–1366. doi:10.1038/onc.2013.81.

Low-dose Arsenic induces chemotherapy protection via p53/NF-κB-mediated metabolic regulation

Suthakar Ganapathy[1,2], **Shaowen Xiao**[1], **Seog-Jin Seo**[1], **Rajuli Lall**[1], **Mei Yang**[1,2], **Teng Xu**[1], **Hang Su**[1], **Miriam Shadfan**[1], **Chul S. Ha**[1], and **Zhi-Min Yuan**[1,2]

[1]Department of Radiation Oncology, Cancer Therapy and Research Center, University of Texas Health Science Center at San Antonio, TX -78229, USA

[2]Department of Genetics and Complex Diseases, Harvard School of Public Health, Boston, MA -02115, USA

Abstract

Most chemotherapeutical drugs kill cancer cells chiefly by inducing DNA damage, which unfortunately also causes undesirable injuries to normal tissues, mainly due to p53 activation. We report a novel strategy of normal tissue-protection that involves p53/NF-κB coordinated metabolic regulation. Pretreatment of untransformed cells with low doses of arsenic induced concerted p53 suppression and NF-κB activation, which elicited a marked induction of glycolysis. Significantly, this metabolic shift provided cells effective protection against cytotoxic chemotherapy, coupling the metabolic pathway to cellular resistance. Using both in vitro and in vivo models, we demonstrated an absolute requirement of functional p53 in arsenic-mediated protection. Consistently, a brief arsenic-pretreatment selectively protected only normal tissues but not tumors from toxicity of chemotherapy. An indispensable role of glycolysis in protecting normal tissues was demonstrated by using an inhibitor of glycolysis, 2-deoxyglucose, which almost totally abolished low-dose arsenic-mediated protection. Together, our work demonstrates that low-dose arsenic renders normal cells and tissues resistance to chemotherapy-induced toxicity by inducting glycolysis.

Keywords

Chemoprotection; p53; NF-κB; Metabolism; Colon cancer

Introduction

Chemotherapies kill cancer cells primarily by inducing DNA damage, which potently activates p53. Abundant evidence indicates that the toxicity caused by DNA-damaging

Correspondance to: Zhi-Min Yuan, MD, Ph.D, Department of Genetics and Complex Diseases, Harvard School of Public Health, 655 Huntington Avenue, SPH Building I, Boston, MA 02115, USA. zyuan@hsph.harvard.edu, Ph: 617.432.2139., Fax: 617.432.2296.

Conflict of Interest

Authors declare no conflicts of interest

anticancer therapy is mainly mediated by p53 (1). Recent studies using mouse models indicate that a temporary suppression of p53 activity can significantly reduce DNA damage-induced cytotoxicity without compromising the tumor suppression function (2, 3), raising a probability of brief p53 inhibition for cancer therapy protection.

The transcription factor NF-κB regulates various genes important for the immune response, cell proliferation, and cell survival (4, 5). During the immune response, cells consume large amounts of glucose and primarily use aerobic glycolysis to produce enough energy to meet the bioenergetics demands of cellular proliferation and survival (6). In addition to its involvement in the immune response, the NF-κB pathway has also been shown to be activated by irradiation-induced DNA damage, but the functional consequences of this response were shown to be multifaceted, as NF-κB was capable of functioning either as a pro-survival or pro-death signal (7). Dynamic crosstalk has been demonstrated between the p53 and NF-κB pathways. Although this crosstalk is highly context dependent and has been shown to function either as antagonistic or cooperative between the two pathways, p53 and NF-κB are considered to overall function against one another to maintain cellular homeostasis (8).

By expanding our recent study indicating that low-dose arsenic can suppress chemotherapeutic drug 5FU-induced p53 activation (9), we exploited the use of arsenic for protection of normal tissues against chemotherapy-associated damages. We show that low-dose arsenic protects sensitive tissues by inducing reciprocal p53 suppression and NF-κB activation, and subsequent metabolic shift. Using colon carcinoma xenograft mouse models, we demonstrate that a brief pretreatment with low-dose arsenic protected selectively normal tissues, but not tumor cells, from 5-Fluorouracil (5FU) induced killing.

Results

A mutually exclusive interaction between p53 and NF-κ B in low-dose arsenic-induced protection

When human fibroblasts were treated with 5FU, a distinct response of p53 and NF-κB was observed. In contrast with p53, which was robustly induced in response to DNA damage (supplemental Fig. 1A), little NF-κB activity was detected in 5FU-treated human fibroblasts, as reflected by a chiefly cytoplasmic p65 distribution (supplemental Fig. 1B). The lack of NF-κB activity in 5FU-treated cells was not due to any defect of this pathway since there was a clear induction of p65 nuclear distribution by TNFα, a known NF-κB activator (supplemental Fig. 1B). This distinct response of p53 and NF-κB led us to test the effect of low-dose arsenic, which we previously showed can inhibit 5FU-induced p53 activation (9). When compared with the control, pretreatment of human fibroblasts with 50 nM arsenic for 12 h resulted in marked suppression of both p53 activation and γH2AX induction by 5FU (Fig. 1A. 5FU versus As+5FU), consistent with what was observed with epithelial cells (9). Interestingly, parallel to this impaired p53 response was NF-κB activation, as indicated by an overt p65 nuclear distribution in arsenic-treated cells (Fig. 1B). Significantly, low dose arsenic-pretreatment was also associated with considerable NF-κB activation in 5FU-treated cells (Fig. 1B). To tie the response of p53 and NF-κB with cellular sensitivity to 5FU, we examined cell survival by performing an apoptotic assay. Consistent with the significantly

diminished γH2AX and p53 induction in arsenic-treated cells, the 5FU-induced apoptosis was considerably reduced (Fig. 1C). Collectively, the data demonstrated an inverse correlation of p53 and NF-κB with cell survival, where p53, but not NF-κB, activation was linked to 5FU-induced cell death while, conversely, low-dose arsenic-induced protection was associated with concerted suppression of p53 and stimulation of NF-κB.

A requirement of functional p53 in low-dose arsenic-induced protection

We further investigated this seemingly opposite response of NF-κB and p53 to arsenic by asking whether suppression of p53 function is necessary for NF-κB activity. Cells were pre-treated with a low dose of Nutlin-3a, a p53 specific activator. Interestingly, under the condition of mild p53 activation, low-dose arsenic-induced p65 nuclear distribution was completely blocked (Fig. 2A, As versus Nutlin 3a+As), suggesting that p53 inhibition is necessary to allow NF-κB activation. Correlated with the NF-κB activity was cellular sensitivity. In Nutlin 3a-treated cells, arsenic was unable to induce protection. The levels of 5FU-induced γH2AX were comparable in the presence or absence of arsenic (Fig. 2B). We further tested the p53 requirement by depleting the p53 expression with siRNA. Indeed, down-regulation of p53 nearly eliminated the difference of cellular sensitivity to 5FU between arsenic-treated and untreated cells (Fig. 2C). We also used a mutant p53-expressing mouse model to validate the *in vitro* findings. In contrast to wild-type p53 mice where arsenic prevented 5FU-induced body weight loss, p53 mutant mice showed little response to arsenic (supplemental Fig. 2). Together, the results indicate that functional p53 is essential for low-dose arsenic-induced protection.

Low-dose arsenic-induced protection is mediated by a metabolic change

Growing evidence indicates that both p53 and NF-κB are involved in regulation of cellular metabolism, where p53 promotes oxidative phosphorylation whereas NF-κB stimulates aerobic glycolysis(10). We tested the possibility that arsenic-induced p53 suppression coupled with NF-κB stimulation may affect cellular metabolism by favoring glycolysis. Indeed, when compared to control cells, an equal number of low-dose arsenic-treated cells exhibited a clear increase of lactate production (Fig. 3A), which was blocked by the addition of 2-deoxyglucose (2-DG), an inhibitor of glycolysis, supporting a glycolytic metabolism. To substantiate this observation, we determined the level of glucose transporters 1 and 3 since the expression of glucose transporters are critical to glycolysis (4, 11). Immunostaining revealed that the levels of GLUT-1 & 3 were indeed considerably induced by arsenic treatment (Fig. 3B). A close temporal correlation with arsenic-induced p65 nuclear localization and GLUT-3 induction suggested a NF-κB mediated regulation (supplemental Fig. 3). Apart from GLUT-3, NF-κB was reported to induce HIF1α (5). Interestingly, arsenic induced not only a clear increase of the protein abundance but also nuclear distribution of HIF1α (Fig. 3C). Treatment with Capsaicin, an NF-κB pathway inhibitor, blocked this effect of low-dose arsenic, consistent with NF-κB-dependent regulation (Fig. 3C).

We also used Nutlin-3a and capsaicin to demonstrate that p53 inhibition and NF-κB stimulation were critical for the induction of GLUT-3 by arsenic (Fig. 3D & E). The effect of capsaicin was further verified by depleting p65 expression with siRNA (supplemental

Fig. 4). Together, our data indicate a functional interaction between p53 and NF-κB in regulation of cell metabolism. By inhibiting p53 activity and permitting NF-κB to function, low-dose arsenic induces glycolysis.

We went on to test whether the observed increase in glycolytic metabolism contributes to the arsenic-induced resistance to 5FU. Two independent approaches, limiting glucose supply or 2-DG, were used to inhibit glycolysis. Low glucose cultures completely lost arsenic-induced protection as evidenced by a comparable level of apoptosis induction by 5FU in lymphocytes with or without pretreatment of arsenic (Fig. 4A). The requirement of glycolysis was further supported by the use of 2-DG, which nearly completely abrogated arsenic-induced protection (Fig. 4A). The crucial role of glycolysis in arsenic-mediated protection was also evident when γH2AX induction was analyzed in fibroblasts (Fig. 4B–D). We further substantiated the data derived from 2-DG by using RNAi by knocking down the expression of lactate dehydrogenase (LDH), an enzyme essential for glycolysis. A result almost identical to that of 2-DG was observed (Fig. 4E), supporting a requirement of glycolysis in arsenic-mediated protection. An important role of the pentose phosphate pathway (PPP) was also tested by depletion of the expression of glucose-6-phosphate dehydrogenase (G6PD), the rate-limiting enzyme of PPP. The arsenic-mediated protection was abrogated in G6PD-deficient cells (Fig. 4F). The immunostaining data in fibroblasts were further validated by the colony formation survival assay (Fig. 4G), supporting a critical role of the glycolytic and PPP pathways in arsenic-induced protection. Collectively, our data support a model in which low-dose arsenic induces a coordinated p53 inhibition and NF-κB stimulation, which upregulated the expression of HIF1α and GLUT-3, leading to a metabolic shift to glycolysis, and it is the glycolytic and PPP pathways that render cells increased resistance to 5FU toxicity.

To test the physiological relevance of low-dose arsenic-induced cellular resistance, we extended our study to mice. Immunohistochemistry of the small intestine, a tissue very sensitive to 5FU, indicated an overt increase of the GLUT-3 protein abundance in the arsenic and arsenic plus 5FU, but not the control or 5FU alone treated mice (Figure 5A), consistent with the *in vitro* data. To complement the analysis of GLUT expression, we performed live animal imaging to monitor the uptake of labeled 2-DG. Strikingly, a clear increase of glucose uptake was evident in low-dose arsenic-treated mice. The glucose uptake in the arsenic plus 5FU-treated mice was also considerably increased, albeit slightly lower than that in mice treated with arsenic only (Figure 5B). Inspection of the small intestine crypts morphology revealed a close correlation of glycolysis and protection (Figure 5C). The importance of glycolysis was further supported by a pre-treatment of mice with 2-DG (200mg/kg body weight), which blocked arsenic-mediated protection (Figures 5C).

Low dose arsenic selectively protects normal tissues without affecting the antitumor efficacy of 5FU

We next exploited the distinct p53 status that separates normal tissues from most cancer cells to assess the potential of low-dose arsenic in selectively protecting normal tissues from 5FU-induced injury. For this purpose, we used a colon carcinoma cell line SW-480 to generate a mouse xenograft model. Treatments were initiated when the tumor reached an

average volume approximately 100 mm^3. The mice were pretreated with or without 0.4 mg/kg sodium arsenite for three days before subjected to 5FU treatment. The tumor volume in the vehicle group continued increase with time (Fig. 6A). Low-dose arsenic treatment did not have any detectable effect on tumor growth (Fig. 6A). 5FU treatment (30mg/kg body weight i.v.) daily for one week resulted in marked tumor inhibition (Fig. 6A). Significantly, low-dose arsenic pretreatment showed little effect on 5FU-induced tumor suppression, as 5FU-induced tumor regression is indistinguishable in mice that were pretreated with or without low-dose arsenic (Fig. 6A). There was little difference between male and female mice in response to the treatment of 5FU and arsenic (Fig. 6A). Our data thus indicate that a brief pretreatment with low-dose arsenic does not detectably affect the efficacy of 5FU, at least in the human colon carcinoma xenograft mouse model.

To examine whether low-dose arsenic could alleviate 5FU-induced toxicity in these tumor-bearing mice, we monitored body weight change. In contrast to control and low-dose arsenic-treated mice, 5FU-treated mice exhibited a significant loss of body weight (Fig. 6B). This weight loss is most likely caused by 5FU toxicity and not the effect of tumors as we saw almost complete recession of tumors in these animals (Fig. 6A). Remarkably, the 5FU-induced body weight loss was almost completely prevented in both male and female mice by the arsenic pretreatment (Fig. 6B).

To corroborate the result of body weight measurement, we assessed the effect of low-dose arsenic at the tissue level and observed a similar protection. 5FU-induced damage to the small intestine was markedly ameliorated by low-dose arsenic pretreatment (Fig. 6C). The protective effect of arsenic is also evident in the bone marrow. Bone marrow cell exhaustion was clearly observed in 5FU-treated mice. However, this decrease of bone marrow cellularity was considerably alleviated in low-dose arsenic-pretreated mice (Fig. 6D). Collectively, the results demonstrate that a brief treatment with low-dose arsenic is associated with a marked protection of normal tissues without compromising the ability of 5FU to kill carcinoma cells.

Since arsenic has been reported as a carcinogen or co-carcinogen (12), it is of great importance to determine whether the use of arsenic as described aforementioned might increase cancer risk. Ionizing radiation, a classical carcinogen, was used as a positive control and indeed induced a significant increase of incidence of cancer, as reflected by the cancer-associated death (16). In contrast, there was no detectable cancer development in both arsenic-treated and control mice during 12-month period (Fig. 6E), indicating that such a brief use of low-dose arsenic in mice did not detectably increase cancer risk.

Discussion

p53 and NF-κB are two transcription factors important in controlling cell survival or death (13). We demonstrate that cellular fate is determined by an integrated interaction of these two transcription factors. 5FU-induced cell death resulted from p53 activation coupled with little NF-κB activity. Interestingly, low-dose arsenic provoked a very different effect on these two transcription factors by inducing reciprocal p53 inhibition and NF-κB activation. Importantly, p53 suppression seemed to be pre-requisite for NF-κB activation, as shown by

that Nutlin 3a-induced p53 activation blocked low-dose arsenic-induced NF-κB activation. Moreover, the interaction requires a functional p53 as low-dose arsenic failed to stimulate NF-κB activity and was unable to reduce 5FU toxicity when the expression of p53 was depleted. The requirement of functional p53 enabled low-dose arsenic to selectively protect wild-type p53 expressing cells, as demonstrated with the tumor xenograft mouse model in which pretreatment with low-dose arsenic resulted in protection of animals against 5FU-induced acute toxicity to normal tissues without affecting the anti-tumor efficacy of 5FU. This requirement of wild type p53 is significant because p53 is very frequently inactivated in human cancers (10, 13) and the distinct p53 status between normal and tumor tissues enables low-dose arsenic to preferentially protect normal tissues.

A unique feature of arsenic-induced effects is a biphasic dose response: the effects induced by low-dose arsenic are not only different in magnitude from that of high-dose arsenic but also in nature, i.e. cyto-protective versus cytotoxic (12, 14, 15). The protective effects observed in our study with low-dose arsenic are in agreement with published results. We, however, expanded the effects of low-dose arsenic to the functional interaction between p53 and NF-κB in regulation of cellular metabolism. We demonstrate that by suppressing p53 activity and permitting NF-κB to act on the metabolic pathways, low-dose arsenic induced a metabolic shift to glycolysis. NF-κB initiated the glycolytic pathway by up-regulating the expression of *GLUT3* and *HIF1α. GLUT3* encodes the glucose transporter protein GLUT-3, facilitating the uptake of glucose. HIF1α is the master transcription factor known to positively regulate a number of enzymes in the glycolytic pathway. This glycolytic induction is reminiscent of the Warburg effect, which offers the growth and survival advantages(11). We presented multiple lines of evidence to demonstrate that it was the glycolytic and PPP pathways that provided cells or tissues the ability to mount the defense mechanism against 5FU toxicity. Low-dose arsenic treatment failed to protect normal cells or tissues when glycolysis was suppressed by 1) limiting the glucose supply; 2) inhibiting hexokinase activity with 2-DG; 3) knocking down of LDH or G6PD. Considering Arsenic Trioxide being currently in clinic use, a brief treatment with low-dose arsenic has the potential as a novel approach of chemotherapy protection.

Materials and Methods

Cells, Cell culture

Normal human B-cell lymphocytes (Coriell, #GM03798) were maintained in RPMI-1640 supplemented with 10% fetal bovine serum (FBS), L-glutamine, (4-(2-hydroxyethyl)-1 piperazineethanesulfonic acid) HEPES buffer and sodium pyruvate. Human fibroblasts (Coriell, #GM08680) and human colon carcinoma cells, SW-480 (ATCC) were cultured in Dulbecco's modified Eagle's medium (DMEM) supplemented with 10% fetal bovine serum (FBS), L-glutamine, and streptomycin.

Immunofluorescence analysis

For immunofluorescence analysis post 5FU-treatment, human fibroblasts were fixed with 3.7% paraformaldehyde, permeabilized using cold methanol and blocked with 1% BSA. After blocking, cells were incubated with a primary antibody for overnight. The following

primary antibodies were used: anti-phospho γH2AX (Ser139, Cell Signaling Technology, #9718), p53 (1C12, Cell Signaling Technology, #2524), anti NF-κBp65 (abcam, #ab16502), HIF-1α alpha (Novus Biologicals, #NB100-134) anti-Glucose transporter GLUT-1 (abcam, #ab32551), anti-Glucose transporter GLUT-3 (abcam, #ab53095) and DAPI (Santa-Cruz Biotechnology #SC-3598). All fluorescensce conjugated secondary antibodies were obtained from Invitrogen. Nikon TE2000 microscope system was used for imaging analysis.

siRNA mediated gene knockdown

All siRNAs were purchased from Sigma-Aldrich. Multiple sequences of siRNA against each gene were used. siGL2, which targets the luciferase gene in pGL2 construct, was used as the negative control. siRNAs were reverse-transfected at 25 nM using Lipofectamine RNAiMAX (Invitrogen, #13778).

Metabolic assays

The extracellular lactate was measured in the cell culture medium with a lactate assay kit (BioVision, #K667-100). Lactate production was calculated as the difference of lactate concentrations between the medium and cell cultures.

Cell viability and FACs analysis

Cell viability was assessed using the trypan –blue exclusion assay. The percentages of viable cells were counted as follows:

$$\text{Viable cells } (\%) = \frac{\text{Total number of viable cells per ml of aliquot}}{\text{Total number of cells per ml of aliquot}} \times 100$$

An annexin V apoptosis kit (Biovision, #K101-100) was used for the FACS-based assay as per manufacturer's instructions.

Animal study

All animal procedures were conducted in accordance with the Guidelines for the Care and Use of Laboratory Animals and were approved by the Institutional Animal Care and Use Committee (IACUC) at The University of Texas Health Science Center at San Antonio (UTHSCSA). Balb/c mice (6 weeks old) were purchased from Harlan laboratories. Mice were housed under pathogen-free conditions and maintained in a 12 h light/12 h dark cycle, with food and water supplied *ad libitum*. Individual mice were treated with or without sodium arsenite (0.4 mg/kg body weight i.p.) for three days. For live animal image, the animals were injected intravenously through tail vein with 100μl of IRDye 800CW 2-DG (10nmol) 1 h after 5FU-treatment (100mg/kg body weight i.v). A caliper IVIS Spectrum system (Caliper, Alameda, CA) was used to capture images. Throughout this study animals were imaged using the same anesthesia protocol, 2% isoflurane in 100% oxygen at 2.5 L/min. Body temperature was maintained at 37°C by a heated stage. The images were acquired with mice in supine position using the epi-illumination method.

For mouse xenograft experiments, inoculums of 3×10^6 SW-480 cells in 0.1 mL of PBS was mixed with Matrigel at 4°C and then injected into the s.c. space on the right flank of mice.

When tumors reached ~ 0.1cm, mice were randomized into experimental groups for treatments.

Histological and immunohistochemical analysis

Prior to embedding in paraffin, tissue specimens were fixed in 37% formalin and dehydrated. Hematoxylin and eosin staining were performed according to standard procedure. For immunohistochemical analysis, paraffin-embedded sections were deparaffinized with xylene, dehydrated in decreasing concentrations of ethanol. Antigen retrieval was performed in 10mM citrate buffer (pH 6.0). Endogenous peroxidase activity was blocked by treating tissue sections with 3% hydrogen peroxide. Sections were incubated with goat serum to block non-specific antibody binding followed by the incubation with primary antibody. The staining procedure was followed the manufacturer's instruction (ABC staining system, Santa-Cruz Biotechnology).

Statistical analysis

Experiments with cell lines were repeated at least 3 times. Two-way ANOVA was used for statistical analysis. For mouse experiments, the Mann Whitney U test was used for comparisons between different groups.

Supplementary Material

Refer to Web version on PubMed Central for supplementary material.

Acknowledgments

This work was supported by NCI/NIH grants 2 R01 CA085679, R01 CA125144. The authors are grateful to Dr. Gigi Lozano (The University of Texas M. D. Anderson Cancer Center, Houston, TX, USA) for the p53 mutant mice. Mouse imaging was performed by Suresh Prajapati, gratefully acknowledged.

References

1. Gudkov AV, Komarova EA. The role of p53 in determining sensitivity to radiotherapy. Nat Rev Cancer. 2003 Feb; 3(2):117–29. [PubMed: 12563311]
2. Christophorou MA, Ringshausen I, Finch AJ, Swigart LB, Evan GI. The pathological response to DNA damage does not contribute to p53-mediated tumour suppression. Nature. 2006 Sep 14; 443(7108):214–7. [PubMed: 16957739]
3. Hinkal G, Parikh N, Donehower LA. Timed somatic deletion of p53 in mice reveals age-associated differences in tumor progression. Plos One. 2009; 4(8):e6654. [PubMed: 19680549]
4. Oeckinghaus A, Hayden MS, Ghosh S. Crosstalk in NF-kappa B signaling pathways. Nature Immunology. 2011 Aug; 12(8):695–708. [PubMed: 21772278]
5. Ben-Neriah Y, Karin M. Inflammation meets cancer, with NF-kappa B as the matchmaker. Nature Immunology. 2011 Aug; 12(8):715–23. [PubMed: 21772280]
6. Wang T, Marquardt C, Foker J. Aerobic Glycolysis during Lymphocyte-Proliferation. Nature. 1976; 261(5562):702–5. [PubMed: 934318]
7. Tergaonkar V, Perkins ND. p53 and NF-kappaB crosstalk: IKKalpha tips the balance. Mol Cell. 2007 Apr 27; 26(2):158–9. [PubMed: 17466617]
8. Perkins ND. Integrating cell-signalling pathways with NF-kappaB and IKK function. Nat Rev Mol Cell Biol. 2007 Jan; 8(1):49–62. [PubMed: 17183360]
9. Huang YL, Zhang JL, McHenry KT, Kim MM, Zeng WQ, Lopez-Pajares V, et al. Induction of Cytoplasmic Accumulation of p53: A Mechanism for Low Levels of Arsenic Exposure to

Predispose Cells for Malignant Transformation. Cancer Research. 2008 Nov 15; 68(22):9131–6. [PubMed: 19010883]

10. Vousden KH, Ryan KM. p53 and metabolism. Nat Rev Cancer. 2009 Oct; 9(10):691–700. [PubMed: 19759539]
11. Koppenol WH, Bounds PL, Dang CV. Otto Warburg's contributions to current concepts of cancer metabolism. Nat Rev Cancer. 2011 May; 11(5):325–37. [PubMed: 21508971]
12. Lamm SH, Engel A, Kruse MB, Feinleib M, Byrd DM, Lai S, et al. Arsenic in drinking water and bladder cancer mortality in the United States: an analysis based on 133 U.S. counties and 30 years of observation. J Occup Environ Med. 2004 Mar; 46(3):298–306. [PubMed: 15091293]
13. Ak P, Levine AJ. p53 and NF-kappaB: different strategies for responding to stress lead to a functional antagonism. FASEB journal: official publication of the Federation of American Societies for Experimental Biology. [Review]. 2010 Oct; 24(10):3643–52.
14. Andrew AS, Warren AJ, Barchowsky A, Temple KA, Klei L, Soucy NV, et al. Genomic and proteomic profiling of responses to toxic metals in human lung cells. Environ Health Perspect. 2003 May; 111(6):825–35. [PubMed: 12760830]
15. Mahata J, Ghosh P, Sarkar JN, Ray K, Natarajan AT, Giri AK. Effect of sodium arsenite on peripheral lymphocytes in vitro: individual susceptibility among a population exposed to arsenic through the drinking water. Mutagenesis. 2004 May; 19(3):223–9. [PubMed: 15123788]
16. Kaplan HS, Brown MB. A quantitative dose-response study of lymphoid-tumor development in irradiated C57 black mice. J Natl Cancer Inst. 1952 Aug; 13(1):185–208. [PubMed: 14946508]

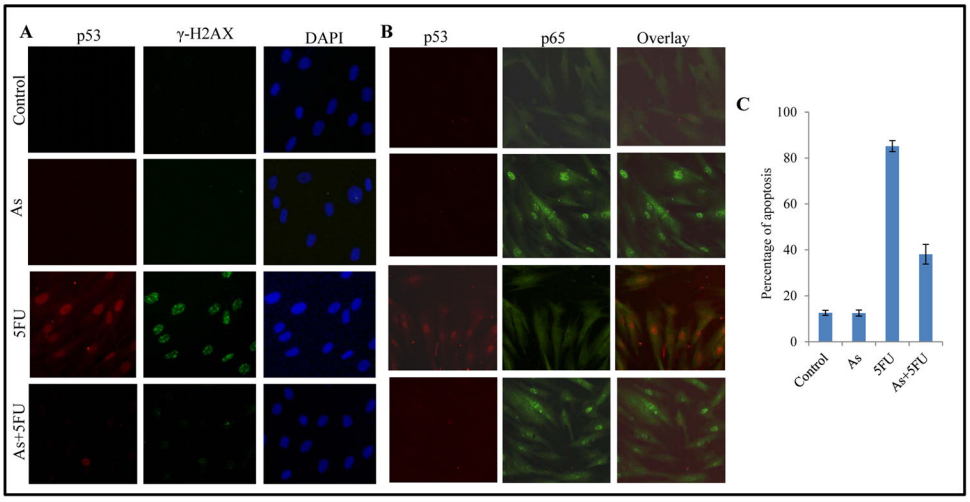

Figure 1.

A distinct response of p53 and NF-κB in low-dose arsenic-induced protection. Human fibroblasts were pretreated with either PBS or 100 nM sodium arsenite for 12 h, followed by 5FU (375 μM) or DMSO. The cells were harvested 1 h after the 5FU-treatment and subjected to either co-immunostaining with p53 and γH2AX (A) or p53 and p65 (B). C, human lymphocytes were pretreated with or without 50 nM sodium arsenite for 12 h. The cells were then exposed to 375 μM 5FU or DMSO. The cells were harvested 12 h later for apoptotic assay by FACS. The numbers are mean ± SD from 3 independent experiments.

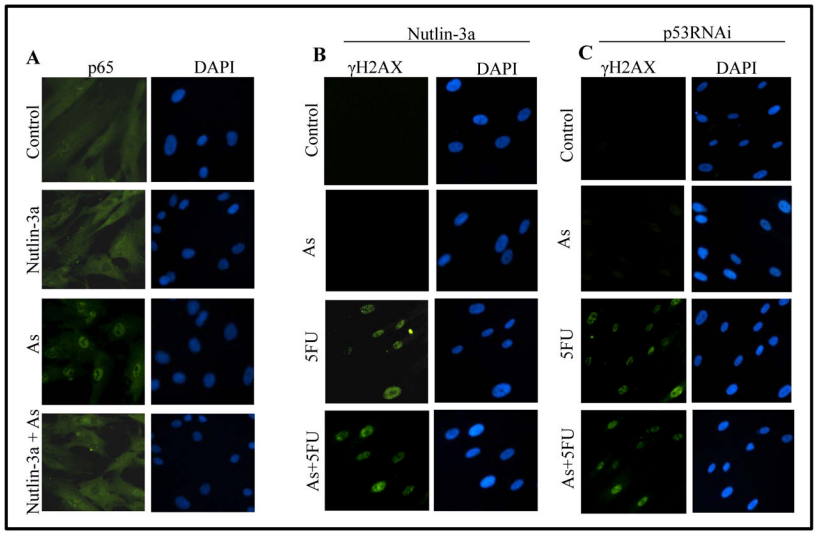

Figure 2.

Requirement of functional p53 in low-dose arsenic-induced protection. A, fibroblasts were pretreated with DMSO (control) or Nutlin-3A (10 μM) for 1 h and then with or without sodium arsenite (100 nM) for 12 h. The cells were harvested for immunostaining with p65 and DAPI couter-staining. B, fibroblasts were treated as in A followed by 5FU-treatment (375 μM) for 1 h. The cells were harvested and stained for γH2AX with DAPI counter-staining. C, fibroblasts were transfected with p53RNAi (the p53RNAi knock down efficiency was determined by RT-PCR and is shown in Supplemental Fig. 5) and subjected to the treatment and analysis as in A.

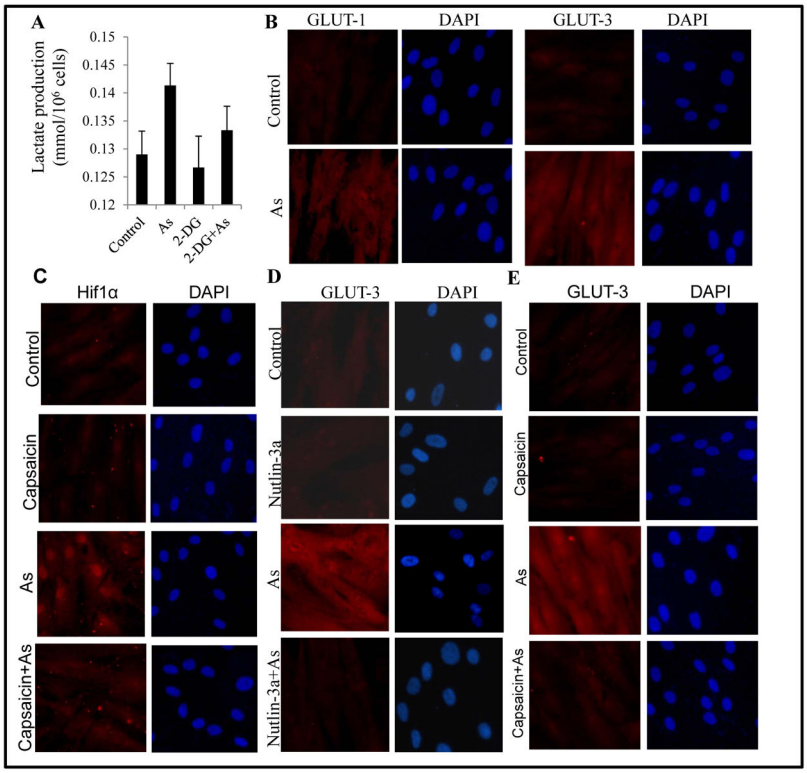

Figure 3.

Low-dose arsenic treatment induces glycolysis via concerted p53 suppression and NF-κB stimulation. A, human fibroblasts were pretreated with DMSO or 2-DG (5mM) for 1 h, followed by either PBS or 100 nM sodium arsenite for 12 h. Culture media were collected for lactate concentration measurement. B, fibroblasts were treated with either PBS or 100 nM sodium arsenite for 12 h. The cells were subjected to immunostaining with anti-GLUT-1 or GLUT-3 antibodies. C, fibroblasts were pretreated with DMSO (control) or Capsaicin (300 μM) for 1 h, followed by arsenic for 12 h. The cells were harvested and immunostained with HIF1α and DAPI. D, fibroblasts were pretreated with DMSO (control) or Nutlin-3A (10 μM) for 1 h and then arsenic as described in C. The cells were subjected to immunostaining with anti-GLUT-3 and DAPI. E, fibroblasts were pretreated with DMSO (control) or Capsaicin (300 μM) followed by arsenic as described in C. The cells were immunostained with GLUT-3 and DAPI.

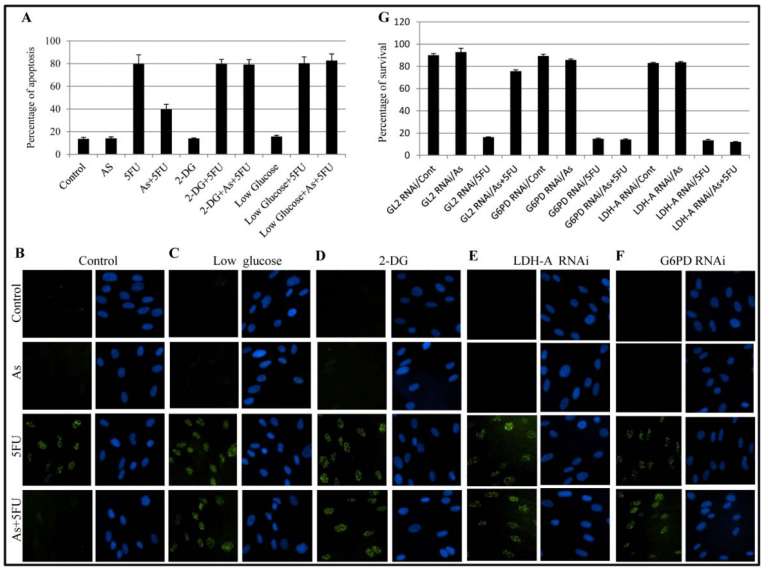

Figure 4.

Glycolysis is essential for low-dose arsenic-mediated protection. A, human lymphocytes were cultured in normal (25 mM glucose) or low glucose (2 mM) media, treated as in Fig. 1C and subjected to apoptotic assay. Lymphocytes were pre-treated with 2-DG (5mM) for 1 h prior to addition of 5FU and then analyzed as in Fig. 1C. Human fibroblasts were cultured in either normal glucose (25 mM) (B) or low glucose (2 mM) (C) media, treated with or without 100 nM sodium arsenite followed by 5FU (375 μM). The cells were fixed 1 h after the 5FU-treatment and immunostained with γH2AX. D, fibroblasts were pre-treated with 2-DG 1 h and subject to the treatment and analysis as in 1C. Fibroblasts were transfected with either LDHA RNAi (E) or G6PD RNAi (F). The RNAi knock down efficiency was shown in the supplemental Fig. 5. The cells were subjected to the treatment as described in B at 48 h post-transfection. G. Fibroblasts were transfected with either control RNAi (GL2RNAi), LDHARNAi or G6PDRNAi. The cells were treated with 100 nM sodium arsenite 48 h post-transfection for 12 h. Cellular sensitivity to 5FU was assessed by performing a colony formation survival assay. The numbers are mean ± SD from 3 independent experiments.

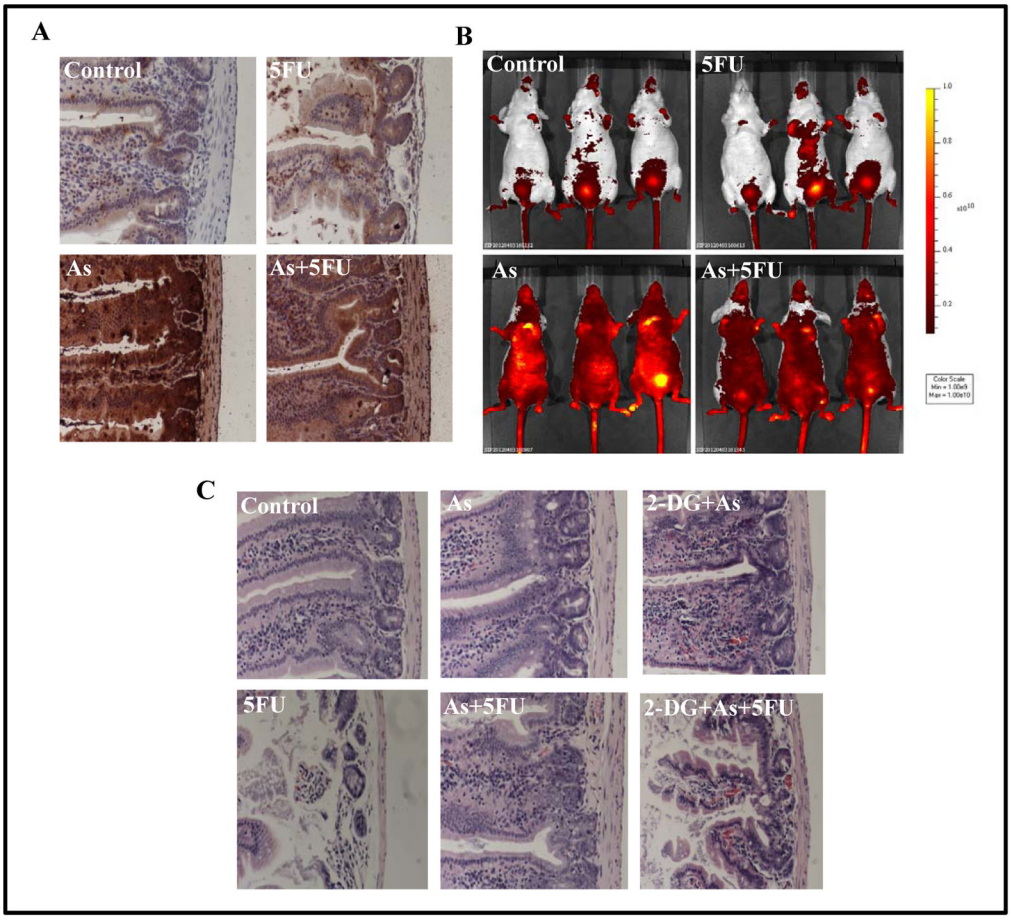

Figure 5.

The *in vivo* study of the low-dose arsenic-induced glycolysis. A, all animal procedures were performed in accordance with a protocol approved by the UTHSCSA Animal Care and Use Committee. Balb/C mice (4–6 weeks) purchased from Harlan laboratories and maintained on a 12 h light/12 h dark cycle, with food and water supplied *ad libitum* were pretreated (intra-peritoneal injection) with or without sodium arsenite 0.4 mg/kg body weight for consecutive 3 days. The animals were then treated with 5FU (100 mg/kg body weight) or DMSO and harvested 24-h later. The small intestines were harvested and the expression of GLUT-3 was examined by immunohistochemical staining. B, Mice were treated as in A and live animal imaging was performed using a procedure described in materials and methods to monitor the uptake of labeled glucose. The optical images are shown. C, mice were treated as in A. 100 μl saline or 2-DG (200mg/kg body weight) was given via i.v. 12 h prior harvesting. The small intestines were harvested and stained with H&E.

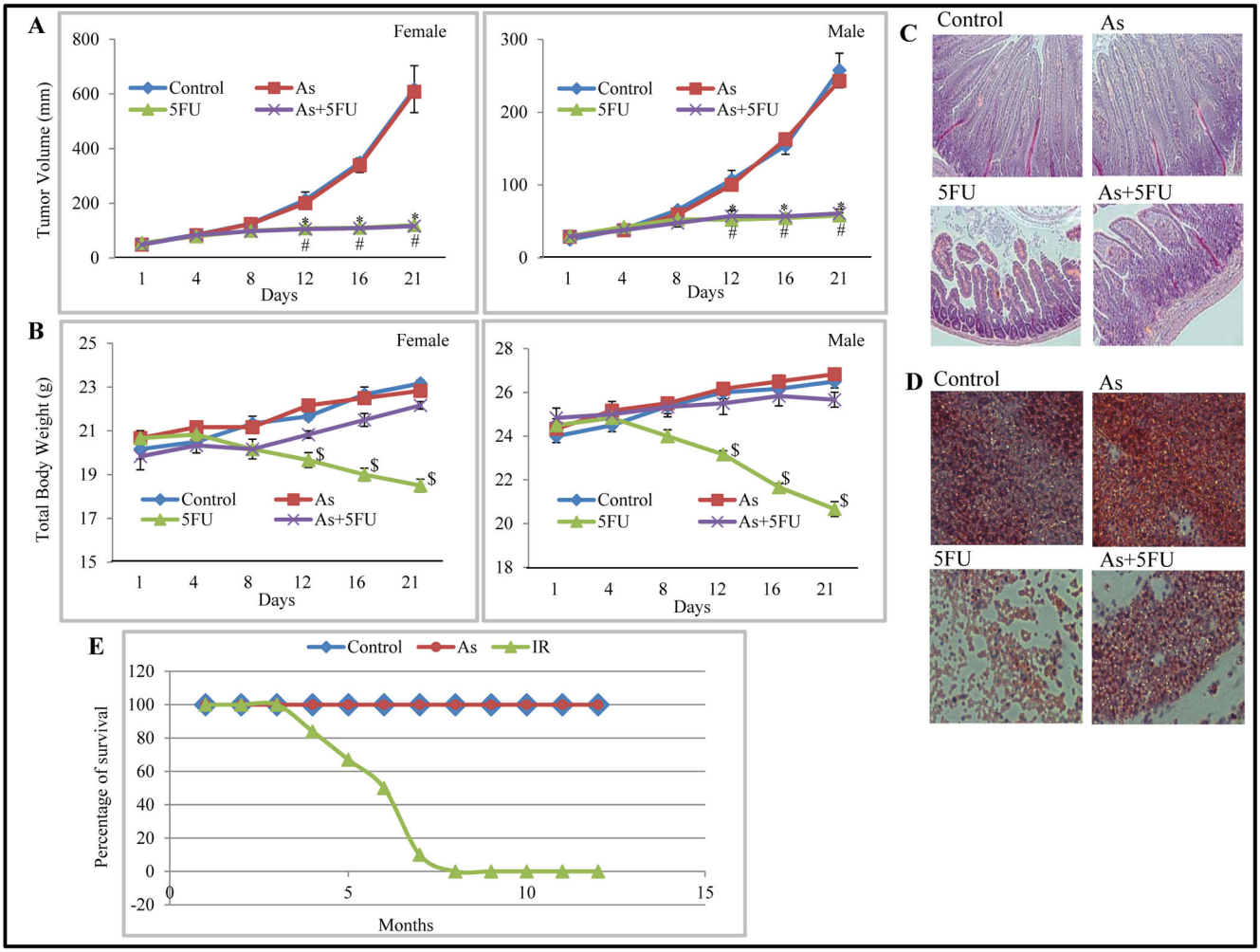

Figure 6.

Low-dose arsenic selectively protects normal tissues without affecting the antitumor efficacy of 5FU. Athymic nude mice (Balb/c$^{nu/nu}$, 4–6 weeks old) were from Harlan laboratories. Human colon carcinoma cell line SW-480 (cells as a 50% suspension in matrigel) as 3 million cells per mouse in a final volume of 100 μl were injected subcutaneously at right flank of Balb/c nude mice. When the average tumor volume reached about 100 mm^3, mice were randomized into following groups; control; arsenite only; 5FU only; arsenite and 5FU. For arsenite pretreatment, mice were treated with sodium arsenite (0.4 mg/kg body weight) for 3 days (Day 0–3). Mice were then treated with either 5FU (30mg/kg body weight) via i.v. daily for one week (Day 4–10). Tumor volumes were measured every four days. Tumor volume was calculated using the equation: (volume = length × width × depth × 0.5236 mm^3). Two independent experiments were done and the tumor volumes are means ± SE from total of 10 mice per group A (* and # are significantly different from control, $P<0.05$). B. Body weight of the mice as described in A was monitored throughout the experiment. The numbers are means ± SD from two independent experiments with total of 10 mice per group ($ is significantly different from control, $P<0.05$). At the completion of the experiments mice were sacrificed by cervical decapitation.

Tissue samples were harvested for histology experiments. H&E staining were performed. Representatives of H&E staining of the small intestine (C) and bone marrow (D) were shown. E. Balb/c mice were treated with PBS or sodium arsenite (0.4 mg/kg body weight) for three days. Third group of mice were treated with ionizing radiation at a dose of 2 Gy for total of 3 doses (6Gy). The animals were monitored for 12 months for tumor development and survival.